# Effect of periodic melting on geochemical and isotopic signals in an ice core from Lomonosovfonna, Svalbard

V. A. Pohjola,[1] J. C. Moore,[2] E. Isaksson,[3] T. Jauhiainen,[2] R. S. W. van de Wal,[4] T. Martma,[5] H. A. J. Meijer,[6] and R. Vaikmäe[5]

Received 9 November 2000; revised 16 July 2001; accepted 26 July 2001; published XX Month 2002.

[1] We examine the quality of atmospherically deposited ion and isotope signals in an ice core taken from a periodically melting ice field, Lomonosovfonna in central Spitsbergen, Svalbard. The aim is to determine the degree to which the signals are altered by periodic melting of the ice. We use three diagnostics: (1) the relation between peak values in the ice chemical and isotopic record and ice facies type, (2) the number of apparent annual cycles in these records compared with independently determined number of years represented in the ice core, and (3) a statistical comparison of the isotopic record in the ice core and the isotope records from coastal stations from the same region. We find that during warm summers, as much as 50% of the annual accumulation may melt and percolate into the firn; in a median year this decreases to ~25%. As a consequence of percolation, the most mobile acids show up to 50% higher concentrations in bubble-poor ice facies compared with facies that are less affected by melt. Most of the other chemical species are less affected than the strong acids, and the stable water isotopes show little evidence of mobility. Annual or biannual cycles are detected in most parameters, and the water isotope record has a comparable statistical distribution to isotopic records from coastal stations. We conclude that ice cores from sites like Lomonosovfonna contain a useful environmental record, despite melt events and percolation and that most parameters preserve an annual, or in the worst cases, a biannual atmospheric signal. *INDEX TERMS:* 1620 Global Change: Climate dynamics (3309), 1827 Hydrology: Glaciology (1863), 1863 Hydrology: Snow and ice (1827), 3344 Meteorology and Atmospheric Dynamics: Paleoclimatology; *KEYWORDS:* ice cores, snowmelt, water isotopes, ice chemistry, percolation in firn

## 1. Introduction

[2] A major problem with extracting climatic and environmental records from ice cores taken from ice fields situated below the dry firn zone [*Benson*, 1961] is the postdepositional altering of the atmospherically deposited strata by the movement of water through the ice column ("ice" here refers to ice matrix composed of different facies snow/firn/ice). Percolation of water during warm events, originating either from rain or from melting of the ice pack, will tend to diffuse downward and advect any chemical or physical signal in the ice strata. Diffusion, in this respect, is the attenuation of an atmospherically deposited layer by percolating meltwater. The warmer the site, the greater the destruction of the signal through diffusion [e.g., *Koerner*, 1997]. This has long been a problem for ice core analysis since this alteration of the signal seems to preclude the possibility of recovering high-resolution records outside cold high-altitude or high-latitude ice fields. Since the ultimate mission is to capture regional and global climatic and environmental changes, the percolation problem restricts the records of change to a few remote and climatically extreme regions of Earth.

[1]Department of Earth Sciences, Uppsala University, Uppsala, Sweden.
[2]Arctic Center, University of Lapland, Rovaniemi, Finland.
[3]Norwegian Polar Institute, Polar Environmental Centre, Tromsø, Norway.
[4]Institute of Marine and Atmospheric Research, Utrecht University, Utrecht, Netherlands.
[5]Institute of Geology, Tallinn Technical University, Tallinn, Estonia.
[6]Centre for Isotope Research, Groningen University, Groningen, Netherlands.


0148-0227/02/2000JD000149$09.00

[3] *Koerner* [1997] showed in a review that ice cores from most Arctic sites exhibit at least 50% of the ice column as clear ice, formed by melt/infiltration/refreeze layers, with the remaining bubbly ice formed by firnification processes with little or no infiltrated water (see Table 1 for a fuller description of the ice terminology used here). This ratio between ice (in lengths of meters water equivalent (mwe)) affected by melting and ice not affected by melting is used as a melt index [*Koerner and Fisher*, 1990]. The higher the melt index, the larger the portion of melt per accumulated mass that affects the site [*Koerner and Fisher*, 1990]. Runoff from the column may occur if the column is fully wetted, which is usually the case close to the firn line (note that the firn line is a dynamic boundary, and in some extremely warm years or warm periods the firn line may migrate high up in an ice field). For example, *Tarussov* [1992] estimated that the effective percolation depth in Austfonna, northeastern Svalbard, was between 2 and 5 m. This means that a signal will be vertically smoothed over this depth, so that to estimate the original strength of the atmospherically deposited signal, a sample would need to be averaged over a thickness of >2–5 m. Austfonna has an average accumulation rate of ~0.5–0.8 mwe $yr^{-1}$ [*Pinglot et al.*, 1999]. This implies that the temporal resolution in the ice core cannot be greater than several years. Preliminary results from chemical analyses from two Japanese ice cores taken on Austfonna in 1998 and 1999 indicate that water percolation has disturbed the record (O. Watanabe, personal communication, 2000).

[4] The melt index of Austfonna was determined by *Koerner* [1997] to be 67%. In an ice core with a melt index <5% from Agassiz Ice Cap, *Koerner et al.* [1999] found the chemical signals to be well preserved in the ice stratum. In Penny Ice Cap, with an average melt index of ~50%, *Grumet et al.* [1998] suggest that the atmospheric signals were preserved with annual to biannual

**Table 1.** Description of Structure Classification and Assigned Density[a]

| Classified Ice Facie | Description | Assigned Density, kg m$^{-3}$ |
|---|---|---|
| 2 | Snow | 350 |
| 3 | Coarse-grained snow | 410 |
| 4 | Fine-grained firn | 530 |
| 5 | Firn | 630 |
| 6 | Coarse-grained firn | 730 |
| 8 | Bubbly ice | 860 |
| 8.5 | Diffuse | 885 |
| 9 | Clear ice | 910 |

[a] Clear ice is devoid of air bubbles, bubbly ice has a large bubble frequency, and diffuse ice has a low amount of bubbles; often large bubbles arranged in arrays. In *Shumskii*'s [1964] terminology these ice types would be (1) infiltration congelation ice, (2) infiltration ice, (3) primary recrystallization ice. We have chosen texture-based terminology in favor of Shumskii's genetically based terminology since visual observation was the basis for categorizing the ice. The value of the assigned density for each facie is based on density measurements from shallow cores 8 and 9 (Figure 1) and from three shallow cores taken on the summit in 1999 (H. Samuelsson, personal communication, 2000). Bubbly ice is, by definition, only present at depths below the firn-ice transition at 29m. The ice facie 1, fresh snow, was not present at this site.

resolution. The results from the Agassiz and Penny Ice Caps show that signals are preserved when there is little or moderate percolation within an ice pack. In this work, we qualitatively and quantitatively analyze the chemical and physical record of the upper quarter (0–36 m) of an ice core taken from the summit of the ice field Lomonosovfonna, Svalbard, to determine the alteration of the stratigraphic record by percolating water.

## 2. Ice Core Site, Climate, and Melt Potential

[5] In May 1997 a 121.6-m-deep ice core was retrieved from the summit of Lomonosovfonna, the highest ice field in Svalbard (Figure 1). The drill site was 1255 m above sea level (asl), and the core was drilled almost to the bed, with poor core quality stopping the drilling a few meters from the bed. After retrieval the core was structurally logged and then sampled and processed for water isotopes and for ice chemistry in 5-cm increments (see *Isaksson et al.* [2001] for detailed information on drill site, drilling, sampling, and analytical methods used). Using the structural record from six shallow ice cores taken in the same year as the summit core [*Isaksson et al.*, 2001], we estimate the boundaries for the different snow zones following *Benson* [1961]: The snow line is

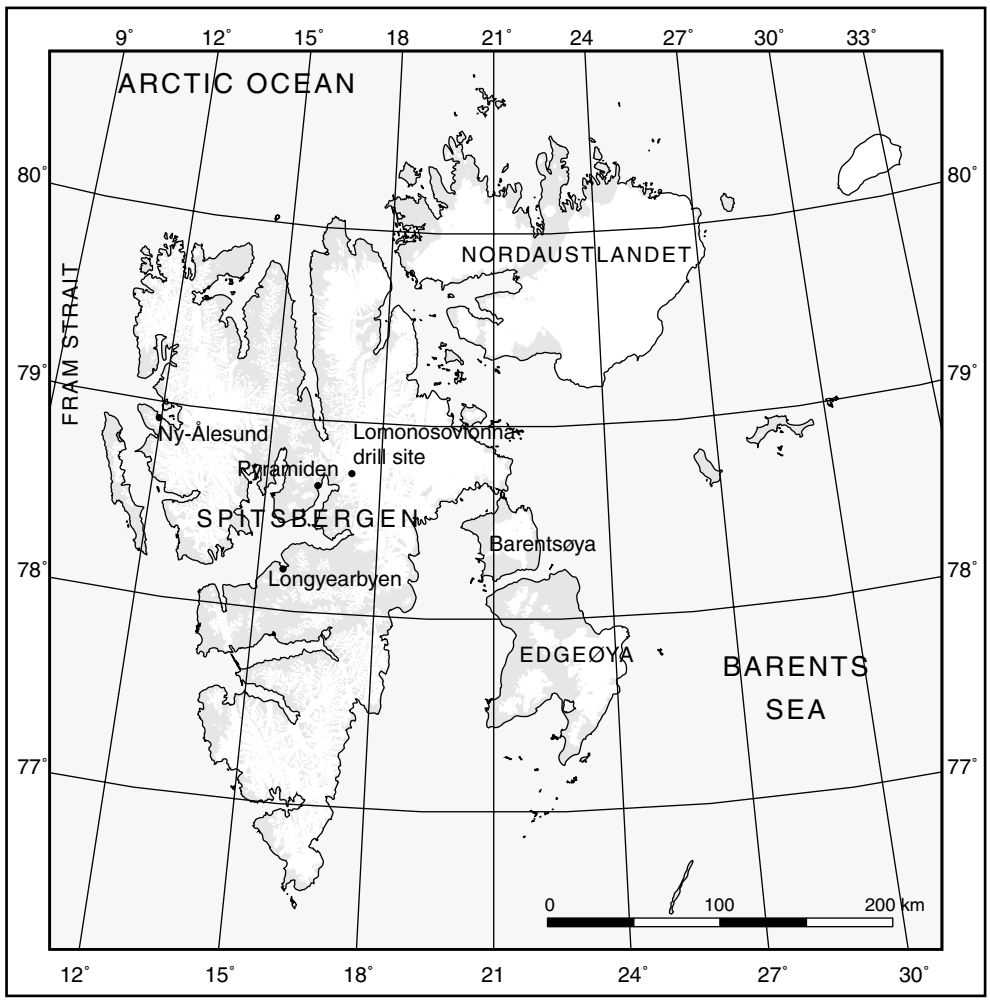


a)

**Figure 1.** (a) The Svalbard archipelago and (b) the ice field Lomonosovfonna. The ice core site is marked in Figure 1a as 10. The numbers 4–9 mark positions of shallow cores extracted contemporaneously with the 121.6-m core at site 10.

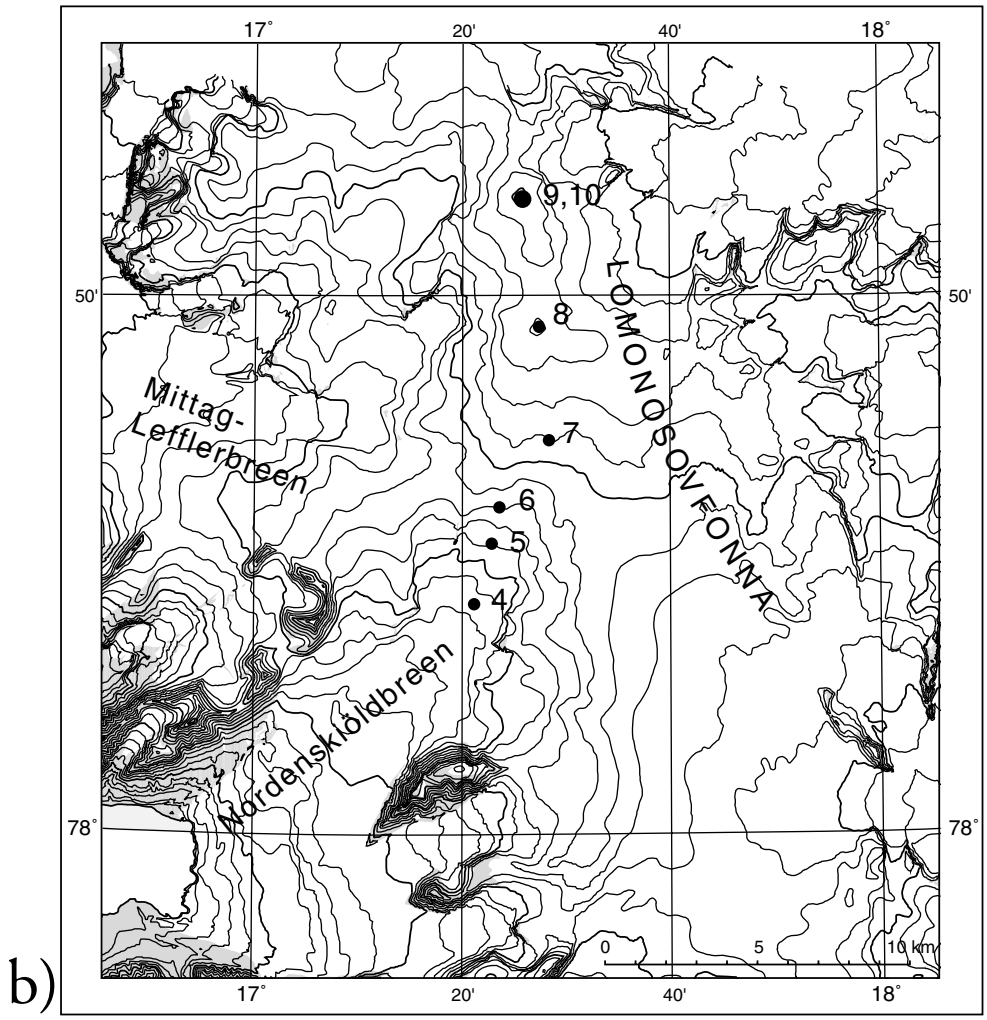


b)

**Figure 1.** (continued)

700–800 m asl, the wet snow line is 950–1050 m asl, the average equilibrium line is somewhere between 500 and 600 m asl, and the dry snow line will probably only be present on the ice field in anomalously cold periods.

[6] The 0- to 36-m interval of the core corresponds to 27.3 mwe on the basis of ice density estimates (see section 3). Using the average accumulation rate for 1963–1997 of 0.36 mwe $yr^{-1}$ derived from the depth of the 1963 β activity peak [*Pinglot et al.*, 1999] implies that the 36-m depth corresponds to circa 1920 A.D., assuming a constant accumulation rate through this part of the core.

[7] Lomonosovfonna has been ice cored twice earlier by Soviet expeditions: a 200-m core in 1976 [*Gordienko et al.*, 1981] and a 220-m core in 1982 [*Zagorodnov et al.*, 1984]. Both cores were drilled a few hundred meters below the summit. Structural studies of the 1982 core gave an average melt index of 34% [*Zagorodnov*, 1998]. Structural observations of the 1997 summit core gave an average melt index of 41% over the whole core length, with a higher index of 55% over the upper 36 m of the core.

[8] An average melt index of 50% over an annual layer indicates an average melt of 33% of the annual accumulation. Thus the calculated firn density of an annual layer is ~500 kg $m^{-3}$ and has a porosity of ~50%. If one third of the annual layer melts and fills the pores in the middle third of the ice and freezes there, then this part of the annual layer will form clear ice (or diffuse ice, depending on the initial porosity and wetting of the firn pack). The upper half of the annual layer will then contain two thirds of the water, while the lower one third is still firn with ~50% porosity. This results in the annual section having a melt index of 50% in the surviving ice pack with 50% clear ice and 50% firn that, with time, will form bubbly ice. With 50% melt the melted firn would fill all pores with the percolating water in the lower half of the section, and the result would be a thick ice layer, or ~100%, in the melt index.

[9] The climate of Lomonosovfonna is not well known. The average near-surface temperature for Lomonosovfonna was estimated as −12.5°C by Soviet expeditions at 1020 m asl [*Zagorodnov*, 1988] (data available from the National Geophysical Data Center). Logging of the borehole temperature profile in the summit borehole showed an average temperature of −2.8°C and a 10-m temperature of approximately −2.3°C. The ~10°C difference between average air temperature and average ice temperature is large. Most of this difference is likely due to energy supplied as advective latent heat from percolating water into the ice column [e.g., *Pfeffer and Humphrey*, 1996].

[10] Unlike most Arctic ice fields a relatively long temperature record exists near Lomonosovfonna. The Svalbard Airport temperature record, which is a composite record synthesized from several instrumental records in and around Longyearbyen, located ~80 km southwest of the core site (Figure 1), extends back to 1911 [*Nordli et al.*, 1996]. To tie the Longyearbyen record to the drill site, an automatic weather station (AWS) was installed at the summit in spring 1999. Owing to heavy rime accumulation, the AWS only gave a 3-day record. Using hourly averages of these 3 days of data from the summit, radiosonde data from Ny-Ålesund (Figure 1), and

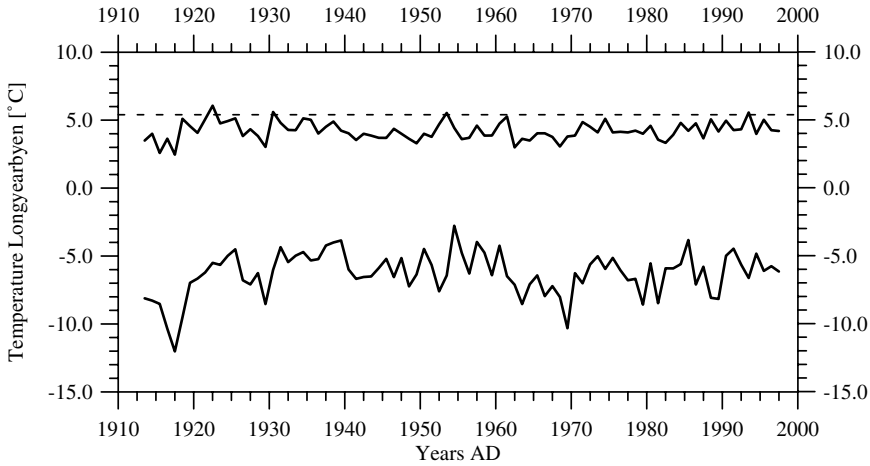


**Figure 2.** The annual average (lower curve) and the summer (June, July, and August) average (upper curve) temperatures for Longyearbyen during 1913–1997. The dashed line shows the estimated sea level temperature at which melting would occur at Lomonosovfonna summit, calculated using the Svalbard Airport monthly temperatures and a constant lapse rate of 0.44°C 100 $m^{-1}$.

temperature data from other central Spitsbergen climate stations (Ny-Ålesund, Longyearbyen, Drönbreen, and Kongsvegen), an average lapse rate of 0.44°C 100 $m^{-1}$ can be established for the area (P. Calanca and J. Sedlacek, personal communication, 2000). Figure 2 shows the annual and summer (June, July, and August) average temperatures over Longyearbyen and the melting point at the summit of Lomonosovfonna calculated using the average lapse rate. Figure 2 suggests that the highest melt periods during the past 90 years were in the 1920s–1930s, 1950s, and 1990s and that the average summer temperature has been typically well below melting at the summit.

[11] Monthly averages are not optimal for detecting melt events at the drill site, however, since several days of high temperatures can be masked in a monthly average. Using daily averaged temperatures at Longyearbyen from 1976 to 1995 and the lapse rate yields an average of 39 days of melting temperatures each year at the drill site. Figure 3 shows the distribution of calculated melt days per year. The melt days are usually bundled in lengths of 5–10 days. A few occasions show extreme warming, and the longest melting period was 38 days (17 July to 23 August 1991).

[12] Another way to view the melt potential at the drill site using the temperature data is to calculate the positive degree day factor (PDD), the sum of daily averaged temperatures each year >0°C [*Braithwaite*, 1995]. PDD at Lomonosovfonna summit, calculated again from the daily averaged Longyearbyen record, ranges from 21°C $d^{-1}$ for the coolest summer (1987, 21 melt days) to 118°C $d^{-1}$ for the warmest summer in the record (1990, 58 melt days).

[13] To quantify the PDD in terms of melting, we use the melt capacity of snow as a function of PDD, which we take as 4.4 mm snow $°C^{-1}$ $d^{-1}$ or as 1.4 mm water $°C^{-1}$ $d^{-1}$, an average from a number of studies [*Braithwaite*, 1995] (Table 2). For the warmest summer in the 1976–1995 record this gives a melt of 0.17 mwe, and for the median year it gives 0.10 mwe. As the average accumulation rate on the Lomonosovfonna summit is 0.36 mwe $yr^{-1}$, this corresponds to 47% melt in the warmest year and to 28% the median year. The average annual accumulation rate in the 1982 Soviet core from Lomonosovfonna over the period 1901–1973 was 0.44 mwe $yr^{-1}$ [*Zagorodnov*, 1988] (data available from the National Geophysical Data Center) with a standard deviation of 0.13 mwe $yr^{-1}$. If we assume that the standard deviation in the summit core is similar to the Soviet core, we find that even during the warmest summers most meltwater probably has the capacity to be stored in the annual strata. This is confirmed by results from detailed ice structure analysis in shallow cores from the Lomonosovfonna summit, which indicate percolation lengths in snow shorter than the annual layer thickness (H. Samuelsson, personal communication, XXXX).

[14] To conclude, despite the uncertainties in the methods used here to estimate melt potential, moderate to small amounts of melt are likely at the drill site. It is not likely, however, that the meltwater moves beyond the annual strata.

## 3. Relation Between Ice Layers and Chemical and Isotopic Records

[15] The first diagnostic we use to investigate potential core alteration is to compare specific signatures in ice chemistry and water isotopes in parts of the ice core with high melt indices with

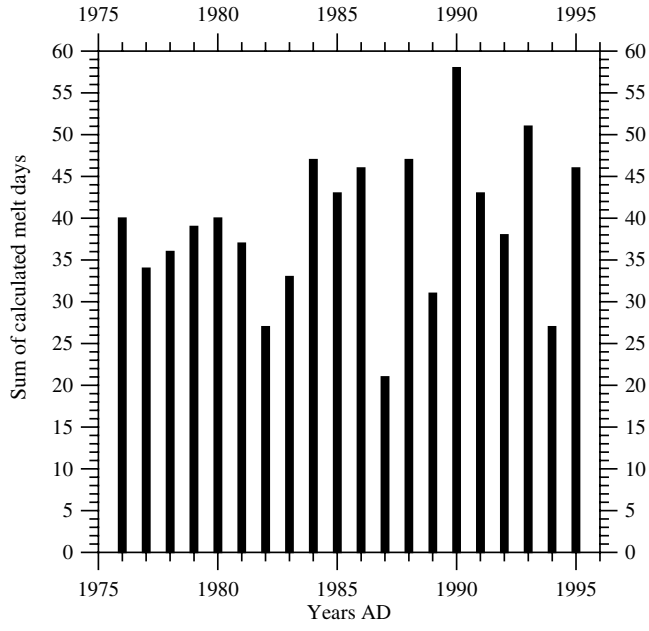


**Figure 3.** Sum of melt days at Lomonosovfonna summit each year, calculated from daily average temperatures at Svalbard Airport during 1976–1995 and from a lapse rate of 0.44°C 100 $m^{-1}$. The average number of calculated melt days at the ice field is 39 d $yr^{-1}$.

**Table 2.** Normalized Distribution of Ionic Concentrations With Respect to the Different Ice Facies[a]

| | F | | | BI | | | DI and CI | | |
|---|---|---|---|---|---|---|---|---|---|
| Ion Species | Average Value | Standard Deviation | Number of Samples | Average Value | Standard Deviation | Number of Samples | Average Value | Standard Deviation | Number of Samples |
| $Cl^-$ | 0.68 | 0.67 | 129 | 1.02 | 0.47 | 55 | 1.27 | 0.79 | 149 |
| $SO_4^{2-}$ | 0.62 | 0.47 | 129 | 0.80 | 0.71 | 55 | 1.40 | 1.09 | 149 |
| $NO_3^-$ | 0.53 | 0.43 | 129 | 0.91 | 0.93 | 55 | 1.45 | 1.38 | 149 |
| $NH_4^+$ | 0.90 | 1.64 | 122 | 0.85 | 1.47 | 41 | 1.13 | 0.90 | 141 |
| $K^+$ | 0.80 | 1.66 | 122 | 0.95 | 1.15 | 41 | 1.19 | 1.14 | 141 |
| $Ca^{2\pm}$ | 0.57 | 1.12 | 122 | 1.55 | 2.52 | 41 | 1.21 | 1.78 | 141 |
| $Mg^{2+}$ | 0.66 | 1.38 | 122 | 1.17 | 1.58 | 41 | 1.25 | 1.31 | 141 |
| $Na^+$ | 0.73 | 0.78 | 122 | 1.06 | 0.54 | 41 | 1.21 | 0.84 | 141 |
| $Br^-$ | 0.57 | 0.81 | 129 | 118 | 082 | 55 | 130 | 106 | 149 |
| MSA | 0.80 | 1.70 | 79 | 1.06 | 0.56 | 7 | 1.33 | 1.09 | 47 |
| NA/Cl | 1.05 | 0.48 | 91 | 1.06 | 0.31 | 7 | 0.93 | 0.66 | 60 |
| An/Cat | 0.87 | | 122 | 1.43 | | 7 | 1.45 | | 141 |

[a] The concentrations are normalized to their respective average concetrations. Each species is normalized to its average concentration in parts per billion, giving 1.00, equal to the average value. Na/Cl is the normalized Na/Cl ratio in μeq $L^{-1}$. An/Cat is tha anion/cation ratio calculated from all species in μeq $L^{-1}$ from the table except for $Br^-$ and MSA. F, firn; BI, bubbly ice; DI, diffuse ice; CI, clear ice.

those parts of the core where the melt index is low. The hypothesis here is that during melt events, chemical impurities in the ice column will be readily mobilized, transported, and deposited with the percolating meltwater farther down in the porous ice or firn column, where it refreezes. Thus the altered signal is not an atmospheric one but a signal of the elution efficiency of impurities by the percolating water.

[16] The potential for elution and transposition varies for each chemical species. Previous studies [*Davies et al.*, 1982; *Goto-Azuma et al.*, 1995; *Grumet et al.*, 1998; *Pasteur and Mulvaney*, 1999] have shown that $NH_4^+$ and methanesulfonic acid (MSA) are relatively mobile in ice even at temperatures well below the melting point, moving as vapor or by solid-state diffusion; these species will be smoothed first. Then the strong acids ($HNO_3$ and $H_2SO_4$) are eluted, followed by $Cl^-$ and $Na^+$. This order is probably related to the physical locations of the impurities within the ice matrix: MSA and strong acids may be liquid, or at least located on the outside of the ice grains, while NaCl originates at least in part as cloud condensation nuclei and will therefore to some degree be present in the interior of ice grains.

[17] The processes of melting, transport, and refreezing are different for water isotopes since both water and ice are the same compound in different phases. It is likely, though, that an altered isotopic signal can be detected since the percolating water will be relatively enriched in heavy isotopes. This occurs whether the percolating water occurs as rainwater, which would be enriched in heavy isotopes because they are from a warmer event, or if it occurs as relatively enriched meltwater from the top snow layers formed by isotopically enriched precipitation events in spring or early summer. This more enriched water will refreeze to form the ice layers in the ice column, which then will have a relatively enriched signal compared with parts of the ice column where the firn has not been infiltrated by meltwater. It is generally assumed that an ice crystal is isotopically homogenous [*Souchez and Lorrain*, 1991] and furthermore that there is no isotopic alteration between the melt, which is formed preferably from the surface of the melting crystals and the residual. Here we also assume that the ice pack does not undergo runoff and is not affected by enrichment of heavy isotopes by melt [*Arnason et al.*, 1973].

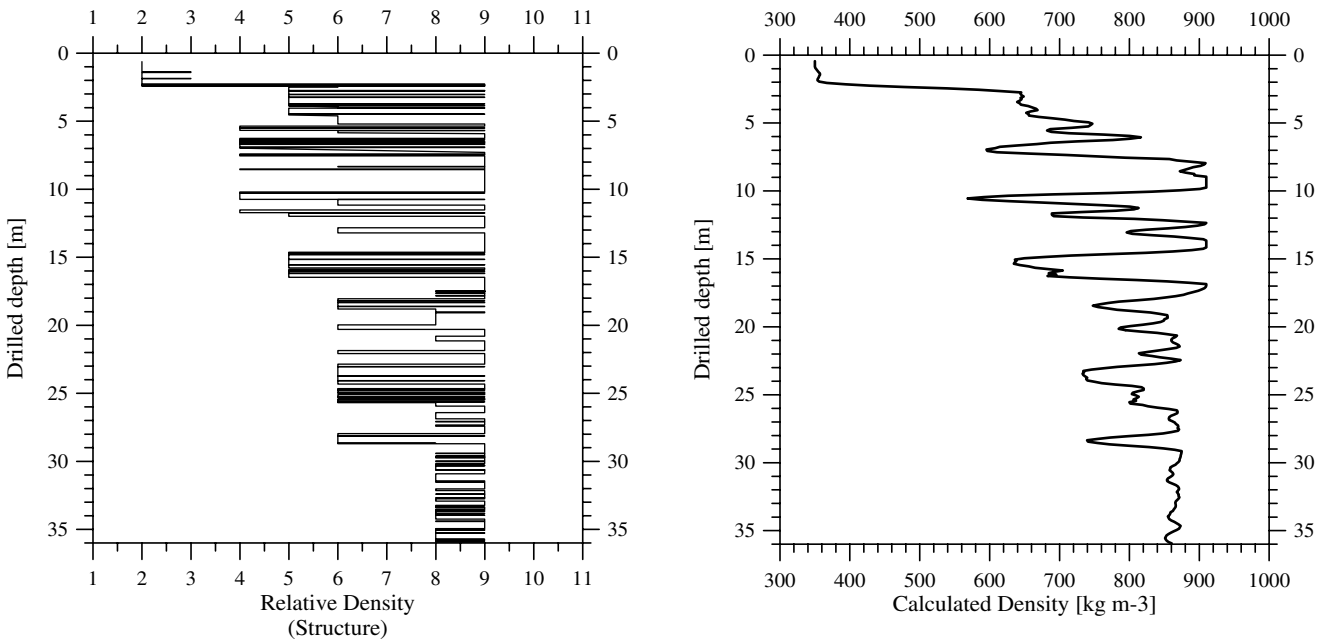


**Figure 4.** (a) Structural view of the ice column with respect to observed ice facies from the ice core face. (b) Calculated density of the upper 36 m.

[18] The method we use is to investigate statistically if differences in isotopic and chemical composition are biased to certain ice facies in the upper 36 m of the ice core. Figure 4 shows the structural distribution and the calculated density of the ice core. The ice structures were recorded to a resolution of 5 mm through visual observations of a flat-cut face of the core. The density is calculated from the structural record. The key to the structural units is given in Table 1. The terminology for facies up to coarse-grained firn are self-explanatory; ''clear'' ice denotes ice devoid of air bubbles; ''bubbly'' ice is ice with many bubbles (this unit is only defined for the 29- to 36-m interval, which is below the firn/ice boundary at 29 m depth); and ''diffuse'' ice represents ice with few, mostly large bubbles, which are often arranged in arrays. A likely genetic account of these facies is that bubbly ice has experienced little or no infiltration of meltwater and has evolved into ice by the firnification processes, the clear ice facie is probably a result of a firn layer with high porosity that has been fully wetted by infiltrating water, perhaps originating as a depth hoar layer with extremely high porosity [*Pfeffer and Humphrey*, 1998], and the diffuse ice facie is most likely the result of an incomplete wetting of a firn pack.

[19] Each structural class was assigned a characteristic density on the basis of measurements of ice density in several shallow cores from the vicinity of the summit core (Figure 1b). The isotopic and chemical data we use come from the upper 36 m of the ice core, and some of the 13 parameters analyzed from the ice core are displayed in Figure 5. All measurements were made using 5-cm subsamples.

[20] Tables 2 and 3 give the statistics, while Figure 6 shows how the different parameters are distributed in the different ice facies. To facilitate comparison between chemical species in Table 2, values for each chemical species are normalized by the respective mean values.

[21] A trend can clearly be seen: The ions most segregated between firn facies and ice infiltrated with water are $NO_3^-$ and $SO_4^{2-}$, which originate from strong acids [*Legrand and Mayewski*, 1997]. The non-sea-salt fraction of $SO_4^{2-}$ (sulphuric acid) accounts for 50–90% of the sulphate signal [*Isaksson et al.*, 2001], suggesting that the strong acids are preferentially eluted in the snow/firn pack on Lomonosovfonna. Next in order of elution are $Cl^-$, $Na^+$, and MSA. As mentioned, MSA is expected to be highly mobile, while sea salt is somewhat less so. $NH_4^+$ and the other cations are less eluted. Some of these cations originate from local, relatively insoluble, crustal species that should be less mobile in the presence of small water flow. $NH_4^+$ is deposited primarily as ammoniated sulphuric acid, as that is the observed form of the aerosol in the atmosphere above Svalbard [*Staebler et al.*, 1999]. However, it seems that the $NH_4^+$ ions are not associated with sulphate species within the ice core, which may indicate segregation of ions during firnification or secondary movement of $NH_4^+$ after deposition. Although $NH_4^+$ ions are relatively easily incorporated in the ice crystal lattice structure, they are known to diffuse rapidly within the solid state, having a solid diffusion coefficient that is several thousand times that of the coefficient of self-diffusion in ice [*Petrenko and Whitworth*, 1999]. The net effect of the varying degrees of elution is to segregate anions more efficiently than cations in water-infiltrated ice facies; this is shown clearly in the anion-cation ratio (Table 2).

[22] In contrast to the ice chemical record the water isotopic records (Table 3) show no significant difference in isotopic composition between the various ice facies, which favors the interpretation of little reorganization of isotopic signals due to percolating water. There is a slight tendency for $\delta D$ to be enriched (less negative) in the bubbly ice facies, which leads to a similar trend in the deuterium excess. As discussed earlier in this section, these results are consistent with ideas on the localization of chemical impurities and with the assumption of homogeneous isotopic ratios throughout the ice crystal. During moderate melt most of the original crystal matrix will stay in its deposited stratum. This suggests that the influence of infiltration ice will be visible primarily in the chemical record rather than in the isotopic record. During percolation events the isotopic strata will be smoothed downward; however, it seems that there is no postatmospheric isotope signal created by this action.

[23] If bubbly ice is derived only from densified firn, then it typically should have ionic and isotopic concentrations similar to the various snow and firn facies. This is the case here; most parameters show more similarity between bubbly ice and firn facies than between bubbly and clear ice although concentrations are higher in bubbly ice than in the firn facies. This may be because bubbly facies are sometimes difficult to distinguish from the infiltration ice facies. This is especially problematic for depths shallower than 29 m, above the firn-ice transition and where pockets of bubbly ice exist, although ice here may have been influenced to some degree by infiltrated water. Another possibility may be temporal trends in concentrations since most of the deeper bubbly ice is older and may have had a different original chemical character. For example, $Ca^{2+}$, which shows the largest concentrations in the bubbly facies, has highest concentrations in the 29- to 36-m interval (Figure 5). The average concentrations are 20.3 ppb (0–29 m) and 61.5 ppb (29–36 m). Making these intervals separate populations gives normalized values of 0.83 for firn and 1.16 for diffuse and clear ice facies in the upper interval and 0.93 for bubbly ice and 1.00 for diffuse and clear ice facies in the lower interval. This shows a distinct temporal trend in concentrations but not in elution. When the trend is eliminated, we find that $Ca^{2+}$ is not severely eluted; on the contrary, is rather conservative.

[24] In summary, the species show a varying degree of elution from firn and bubbly ice into diffuse and clear infiltration ice facies. The species showing greatest differentiation between ice facies were the acid-derived ions $NO_3^-$ and $SO_4^{2-}$, while $NH_4^+$ is the most evenly distributed ionic species; this is probably due to solid-state diffusion within the ice pack after redistribution by percolation. The water isotopes, on the other hand, show very little reorganization. These are plausible results considering the position of the different species with the ice crystal lattice and their potential solubility in water. Quantifying this, the stronger acids have experienced, on average, 40–50% transposition of signal, while for other species, transposition amounts to ~25%.

## 4. Annual Cyclicity

[25] Another way to study the quality of the ice core record is to examine the apparent annual cyclicity of the different parameters. Seasonality in the water isotopic record is well known [*Dansgaard*, 1964]. Seasonal variations in chemical loading are suggested by studies of aerosol composition over Svalbard [*Heintzenberg and Leck*, 1994] which show that both marine and non-sea-salt $SO_4^{2-}$ aerosol peak in winter/early spring as a result of winter storm activity and the Arctic haze pollution. However, $SO_4^{2-}$ can have a more complex annual signal, as it is derived from several different sources and transport paths [*Goto-Azuma et al.*, 1995; *Grumet et al.*, 1998]. MSA aerosol clearly peaks in mid-summer, and concentrations measured in the Lomonosovfonna summit core have a strong correlation with August sea-ice distribution [*O'Dwyer et al.*, 2000]. As MSA is known to be one of the most mobile ions, however, even in ice well below the melting point [*Pasteur and Mulvaney*, 1999] it is not safe to draw conclusions about its current location relative to the isotope signal in the ice. It is clear that marine salts tend to exhibit a winter peak due to greater frequency of storms and enhanced transport efficiency [*Heintzenberg and Leck*, 1994]. Still, other species may exhibit intermittent deposition in Svalbard, such as local sources of dust.

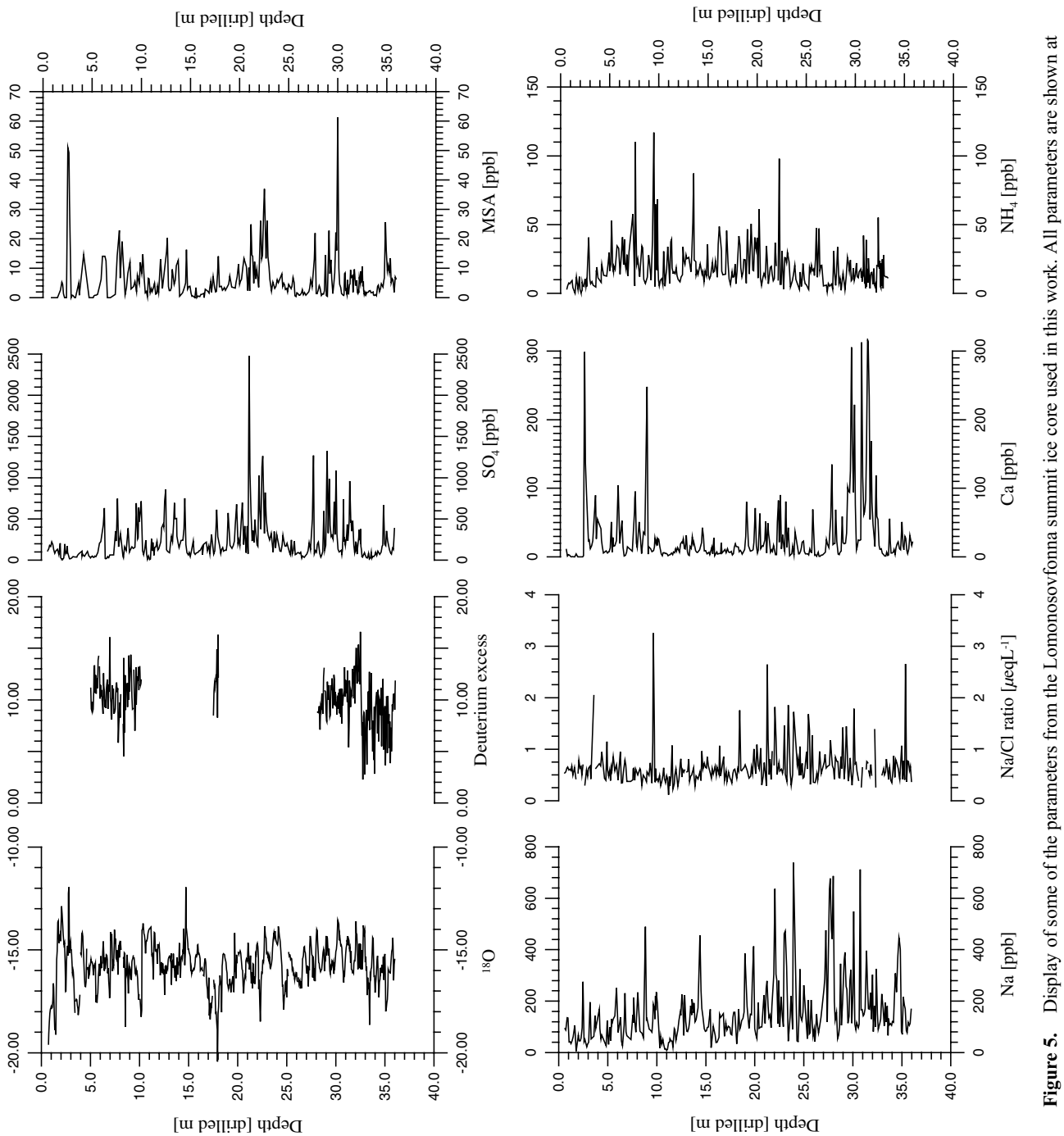


**Figure 5.** Display of some of the parameters from the Lomonosovfonna summit ice core used in this work. All parameters are shown at full sample resolution (no averages).

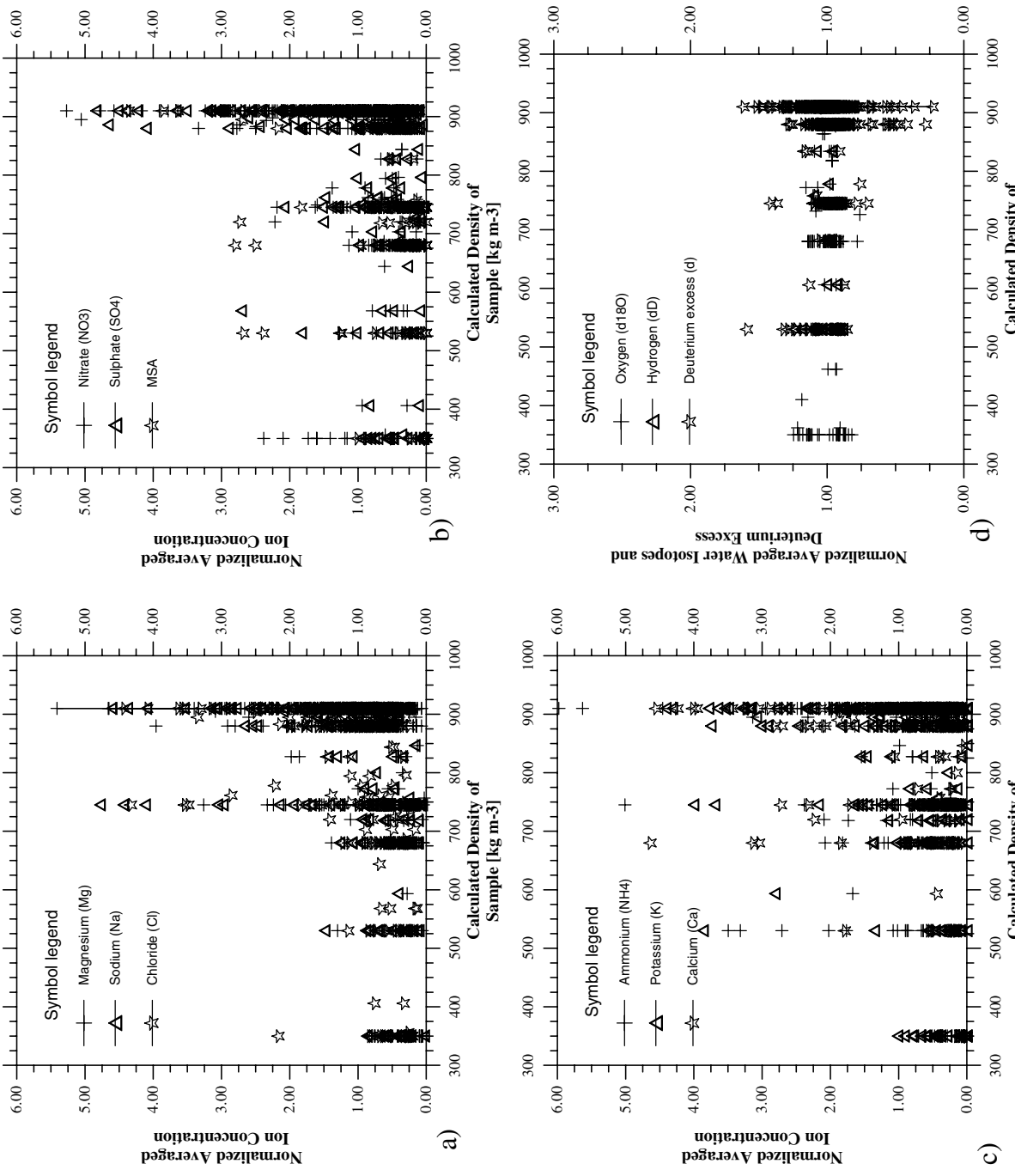


**Figure 6.** The relation between density and ion and isotope concentrations in all samples. Ion and isotope values are normalized by the average value of each parameter.

**Table 3.** Distribution of $\delta^{18}O$, $\delta D$, and Deuterium Excess $d$ With Respect to the Different Ice Facies[a]

| | Firn Facies | | | Bubbly Ice | | | Diffuse and Clear Ice | | |
|---|---|---|---|---|---|---|---|---|---|
| Parameter | Average Value | Standard Deviation | Number of Samples | Average Value | Standard Deviation | Number of Samples | Average Value | Standard Deviation | Number of Samples |
| $\delta^{18}O$ | −15.51 | 1.23 | 250 | −15.51 | 0.97 | 86 | −15.98 | 0.91 | 269 |
| $\delta D$ | −116.67 | 7.03 | 44 | −113.34 | 8.62 | 49 | −117.00 | 7.59 | 137 |
| $d$ | 10.52 | 1.88 | 44 | 8.99 | 2.43 | 45 | 10.39 | 2.35 | 124 |

[a] Values given in ‰ SMOW.

[26] In a study of soluble species in aerosols and in precipitated snow, *Sun et al.* [1998] show that the common species found in dry snow represent, for the most part, the chemical signature in the precipitating air mass; exceptions were $NH_4^+$ and $NO_3^-$ which they found were altered by postdepositional processes. *Beine et al.* [1996], *Hara et al.* [1997], and *Staebler et al.* [1999] give examples of the relationship between the air mass origin and path and of the chemical loading in precipitation over Spitsbergen. These results show that the air mass types vary seasonally due to significant changes in atmospheric circulation in the high Arctic.

[27] However, as we have seen, the distribution of species in the Lomonosovfonna core can be altered by water percolation in the snow pack. In section 3 we concluded that even if all species present are altered to some degree by percolation effects, they still carry a signal that is not completely diffused or smoothed into the ice pack. Clearly, a detectable signal exists, and our hypothesis is that despite reorganization of some percentage of each parameter, the peak values will be detected close to where they were once deposited. Following this, we will examine if there is evidence that annual (or perhaps pseudoannual) cyclicity is preserved in the core.

[28] Investigation of the periodic component of the parameters in Tables 2 and 3 using both traditional Fourier and singular spectrum analyses showed no significant power at the expected annual frequency, assuming a constant average accumulation rate and a simple depth/age model. This lack of an annual cycle can be explained by the large standard deviation in annual (seasonal) accumulation rates, which produces a very smeared-out annual signal in frequency space. As long as we do not have a firm annual chronology for the core, the spectral analyses give little information at high frequencies. Therefore we used a simple cycle-counting routine which calculated the number of cycles in each series by using the change in sign of the second derivative of the parameter with depth as an argument for change of season (with two seasons per annual cycle). Certainly, not every cycle in the record is an annual signal. Some cycles may be produced by intra-annual climatic events, e.g., anomalous. The counting routine has no formal measures of significance, but it is possible to test the robustness of the results by varying two adjustable parameters.

[29] We use two criteria to determine whether a cycle can be counted. The first criterion is the minimum length of a seasonal half cycle. The lower bound is the sample thickness, that is, a seasonal layer needs to be thicker than the 0.05-m core depth. The second criterion is the amplitude that defines a cycle; at a minimum this must be larger than the analytical uncertainty for each parameter. For $\delta^{18}O$ this is the same as the uncertainty of ±0.1‰ SMOW; for the chemical record the minimum is determined by the detection limit and precision, which are different for each species. Both parameters can be adjusted upward, theoretically, without bound. As an average accumulation year, this will contain eight samples per cycle in the ice facie, but years with less accumulation will contain fewer points. The results are shown in Table 4.

[30] The number of cycles were studied in two different depth intervals: 0–36 m, which is the full length of the studied core part, and a control interval between 0 and 18.5 m, which is the part with a known number of 34 annual cycles (1997–1963) [*Pinglot et al.*, 1999]. Both of these intervals were studied using two different search wavelength windows for seasonal layers (half cycles where $\lambda_{seas} > 0.05$ mwe and $\lambda_{seas} > 0.10$ mwe). Most parameters show similar numbers of cycles, except $K^+$, which contains fewer cycles. In the control depth interval, 26–38 cycles were found using the smaller wavelength window. The average number of cycles is 32, which is close to the 34 cycles that should be present if one peak was deposited each year. $NH_4^+$, $Cl^-$, and $NO_3^-$ give 34 cycles, and $\delta^{18}O$ has 38 cycles. This suggests that most parameters have at least a pseudoannual signal preserved in the ice between 0 and 18.5 m, most with small deviations from the real numbers of years. For

**Table 4.** Number of Cycles in the Different Parameters From the Ice Core Record[a]

| | $Cl^-$ | $NO_3^-$ | $SO_4^{2-}$ | MSA | $NH_4^+$ | $K^+$ | $Ca^{2+-}$ | $Mg^{2+}$ | $Na^+$ | $\delta^{18}O$ | Average K |
|---|---|---|---|---|---|---|---|---|---|---|---|
| Detection limit, ppb | 0.3 | 0.5 | 0.7 | 0.3 | 0.5 | 1.2 | 1.2 | 0.6 | 0.5 | 0.1[1] | |
| Precision, RSD% | 0.5 | 1.7 | 2.7 | 6.7 | 5.1 | 15.8 | 2.3 | 2.6 | 2.3 | | |
| RSD determined, ppb | 100 | 50 | 100 | 5 | 15 | 5 | 15 | 15 | 100 | | |
| *Depth of 0–18.5 m, 1963, 34 cycles* | | | | | | | | | | | |
| $\lambda_{seas}$ | 0.05 | 0.05 | 0.05 | 0.05 | 0.05 | 0.05 | 0.05 | 0.05 | 0.05 | 0.05 | |
| Cycles | 34 | 34 | 27 | 26 | 34 | 14 | 31 | 32 | 31 | 38 | 32 |
| $\lambda_{seas}$ | 0.10 | 0.10 | 0.10 | 0.10 | 0.10 | 0.10 | 0.10 | 0.10 | 0.10 | 0.10 | |
| Cycles | 21 | 21 | 22 | 17 | 23 | 8 | 19 | 21 | 19 | 31 | 22 |
| *Depth of 0–36 m, ~1920* | | | | | | | | | | | |
| $\lambda_{seas}$ | 0.05 | 0.05 | 0.05 | 0.05 | 0.05 | 0.05 | 0.05 | 0.05 | 0.05 | 0.05 | |
| Cycles | 83 | 82 | 73 | 67 | 81 | 37 | 67 | 72 | 73 | 79 | 75 |
| $\lambda_{seas}$ | 0.10 | 0.10 | 0.10 | 0.10 | 0.10 | 0.10 | 0.10 | 0.10 | 0.10 | 0.10 | |
| Cycles | 50 | 45 | 46 | 38 | 51 | 28 | 42 | 46 | 44 | 64 | 47 |

[a] The limiting factors for determining a cycle amplitude greater than precision of the parameter. The concentration for which the precision of each species was determined is given in the row below precision. The average number of cycles is calculated for all parameters, excluding $K^+$. The half wavelength $\lambda_{seas}$ (a seasonal layer) is in mwe for each parameter. There is no defined detection limit or precision of $\delta^{18}O$; what is used here as the amplitude criterion is the uncertainty (‰ SMOW) is determination of the $\delta^{18}O$.

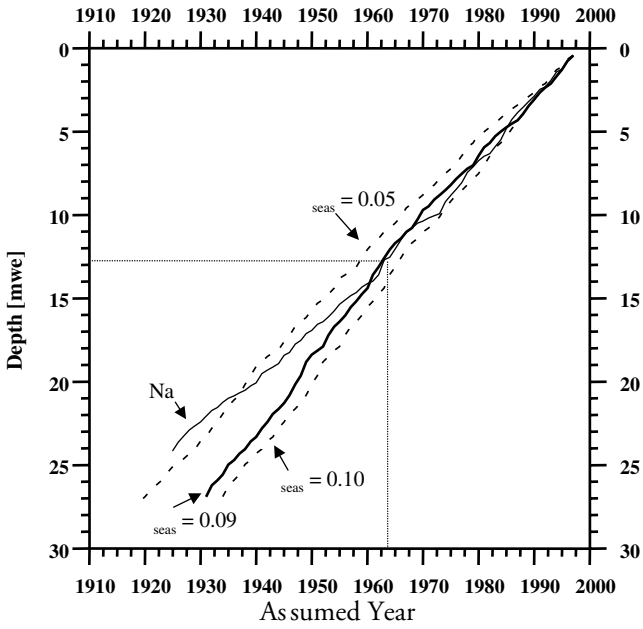


**Figure 7.** The difference in the depth-time relation of the upper 36 meters of the Lomonosovfonna Summit ice core using different search windows for defining a seasonal cycle. The bold and dashed curves are for $\delta^{18}O$, while the thinner curve comes from using cyclicity in sodium (wavelength >0.05 m) as time markers. The dashed curves show the time-depth relation using wavelength >0.10 and 0.05 m. The bold curve is for the criterion wavelength >0.09 m, which gives best result to the known time marker at 12.7 mwe (1963), shown by the dashed curves.

the 0- to 36-m interval we find an average of 75 annual cycles, which would date the 36-m core depth to 1922 A.D.

[31] Using the average number of cycles from the $\lambda_{seas} > 0.05$ mwe window gives an average accumulation rate of 0.40 mwe $yr^{-1}$ over the 0- to 18.5-m interval and an average accumulation rate of 0.36 mwe $yr^{-1}$ in the 0- to 36-m interval. The former is similar to the average accumulation rate between 1996 and 1963 estimated by radioactive horizons [*Pinglot et al.*, 1999]. In addition, measurements of spatial and temporal changes of accumulation rates over the ice field using a ground-penetrating radar along a line between cores 7 and 10 (Figure 1) show that an average accumulation rate of ~0.4 mwe $yr^{-1}$ is a good estimate for the summit of Lomonosovfonna (A. Pälli, personal communication, 2001).

[32] Using $\lambda_{seas} > 0.10$ mwe gives larger accumulation rates (0.58 mwe $yr^{-1}$ for both intervals), which exceeds even the accumulation rate of 0.44 mwe $yr^{-1}$ found from *Zagorodnov*'s [1988] data for the period 1901–1971. Therefore we believe that the search window $\lambda_{seas} > 0.05$ mwe is a better search condition on the basis of logic that some years may have seasonal accumulation layers <0.10 mwe. The standard deviation in annual accumulation rates was estimated to 0.13 mwe $yr^{-1}$ from *Zagorodnov*'s [1988] data. Though accumulation rates are unlikely to be normally distributed, it is clear that some years could have <0.2 mwe $yr^{-1}$ (representing ~45% of the 1963–1997 average accumulation), with a seasonal half cycle of 0.1 mwe.

[33] The $\delta^{18}O$ record generally shows more cycles than the other parameters. The reason for this could be that more intraseasonal excursions were present in the isotope data or that the chemical species have lost a few annual cycles from their record. The $\delta^{18}O$ record also shows the smallest variation in the number of cycles when varying the size of the search window for $\lambda_{seas}$. The distribution of annual cycles with depth for each search window is shown in Figure 7. Since the $\delta^{18}O$ distribution does not match the exact number of annual cycles in the control interval (0–18.5 m), we searched for the optimum search window for $\lambda_{seas}$. We found that using $\lambda_{seas} = 0.09$ mwe gave the exact amount of years in the control period (Figure 7). Extrapolating the series shows that 36 m occurred in 1930 A.D. If the $\delta^{18}O$ cyclicity is annual, this gives an acceptable average accumulation rate of 0.41 mwe $yr^{-1}$ in the depth interval 0–36 m.

[34] To study the robustness of the method, we vary the other parameter, the seasonal amplitude of $\delta^{18}O$, to the control interval 0–18.5 m depth, keeping $\lambda_{seas} = 0.05$ mwe. To arrive at the right number of cycles at 18.5 m (12.7 mwe), the seasonal amplitude search window had to be set as high as 0.23‰. If we used a seasonal amplitude search condition of 1‰, then only 15 of the 34 cycles were found. This indicates that if these cycles are annual, then some of them exhibit small amplitudes and wavelengths in the record. Redistribution of the record by percolating water is an important agent here. Vapor-driven diffusion of the isotopic record also acts to smooth the original signal with time and is a fast enough mechanism to smooth short-scale anomalies, such as individual storms in the winter or spring accumulation period, before melting sets in. Farther down the ice column we have an increasing number of ice layers, which reduces the effectiveness of vapor-driven smoothing [e.g., *Whillans and Grootes*, 1985]. Despite this, the distribution of $\delta^{18}O$ with depth in Figure 5 show that isotopic amplitudes are generally decreasing with depth, a sign that vapor-driven diffusion is an active process.

[35] In conclusion, we find that we are able to detect cyclic variations in isotopic and chemical concentrations that match the number of years we have in the record. This is possible by adjusting the two parameters in a peak-searching algorithm for what we will pass as an annual cycle. The study shows that most parameters have a plausible annual cyclicity, or peak-to-peak deposition, although it is too variable to be found from standard spectral analysis of the core. This fact, combined with the first diagnostic in section 3, strengthens our arguments that atmospheric signals are preserved in the ice core despite percolation events. This study has improved our view of the ice core record since our previous paper [*Isaksson et al.*, 2001].

## 5. Relation Between Climate and Water Isotopic Data

[36] In the preceding two sections we found that seasonal and annual cycles are preserved, for the most part, in both the chemical and water isotopic records and that downward diffusion and dilution by percolating water is not effective enough to remove the atmospherically precipitated signals. The chemical record is more affected than the isotopic record, as seen in section 3. In this section we make a third diagnostic of the quality of the ice core record by investigating the distribution of the water isotopes to find out whether or not the distribution includes climatological information.

[37] If the ice column has been unaffected by melt, then the isotopic record in the ice column would mimic the atmospheric isotopic signal of the precipitation over the ice field through time. If the ice column has suffered from melt, then the atmospheric isotope signal will be distorted both by redistribution of the accumulated signal by percolating water [*Arnason et al.*, 1973] and by alteration of the precipitated isotopic ratio due to fractionation of the isotopic mix during refreezing [*Souchez and Lorrain*, 1991]. As shown earlier, we find that the isotopic signal is not preferably associated with ice facies indicative of melt and that the record still contains what may be viewed as annual cycles. Nevertheless, even if we find annual cycles, they may be altered downward and skewed by percolation. In this

**Table 5.** Statistical Characteristics of the Water Isotope Parameters[a]

| | $\delta^{18}O$ | $\chi_{(\delta^{18}O)}$ | $\delta D$ | $\chi_{(\delta D)}$ | $d$ | $\chi_{(d)}$ |
|---|---|---|---|---|---|---|
| $n$ | 668 | 656 | 270 | 263 | 248 | 237 |
| Mean | −15.7 | 0.5 | −116.1 | 4.3 | 10.1 | 2.1 |
| $\sigma$ | 1.1 | 0.5 | 8.0 | 4.0 | 2.4 | 1.7 |
| $1Q$ | −16.3 | 0.1 | −120.0 | 1.7 | 8.8 | 0.7 |
| $4Q$ | −12.0 | 3.9 | −93.8 | 26.7 | 16.6 | 9.5 |
| $\varsigma$ | −0.4 | 2.7 | −0.7 | 2.2 | −0.4 | 1.2 |
| $\kappa$ | 1.1 | 11.1 | 2.0 | 7.4 | 0.9 | 1.3 |

[a] Deuterium excess was calculated using $d = \delta D - (8\delta^{18}O)$; $\chi$ is the averaged difference from sample to sample as $\chi = Y_z - Y_{z-1}$, where $y$ is the sample and $z$ is the depth; $\varsigma$ is the skewness of each distribution, with high absolute values for a skewed series and low values for less skewed series; $\kappa$ is kurtosis, which has a value of 0 for perfectly distributed Gaussian data but gives higher values for more spiky distribution; $n$ is the number of samples; $\sigma$ is standard deviation; $1Q$ and $4Q$ are the average of the first quartile (the 25% highest numbers) and of the fourth quartile ( the 25% lowest numbers), respectively, of the distribution.

section we first make a statistical analysis of the distribution of the data and then we compare the ice core data with isotope data from continuous sampling of precipitation at coastal stations.

[38] In Table 5 the statistical descriptions of $\delta^{18}O$, $\delta D$, and the deuterium excess $d$ are shown. The table shows the statistics for each parameter, as well as for a series of the sample-to-sample difference $\chi$ for each parameter. The $\chi$ series shows whether the data have smooth transitions between samples or if there are large steps between samples. Figure 8 shows an example of the distribution of the three parameters in the depth interval 2.5–6 mwe.

[39] From the statistics in Table 5 we find that values of kurtosis $\kappa$ are low for $\delta^{18}O$, $\delta D$, and $d$. This suggests that these distributions are closer to Gaussian, with cyclic deposition processes rather than spiky distributions that may indicate redistribution of isotopes by meltwater percolation, at the formation of clear-ice layers. Intra-annual spikes that originally were deposited in the column have been smoothed by vapor-driven diffusion and by percolation, but the longer wavelength signals, such as the annual cycle, are still persistent in the record. If downward transposition of isotopic signals by percolation were the dominant process, then the cycles in the record would be skewed downward and would have peak values located in the clear-ice layers. We did not find any sign of this in section 3, and the relatively low absolute values of skewness (Table 5) suggest that the record is not greatly skewed. The $\chi$ series show low average values for $\delta^{18}O$ and

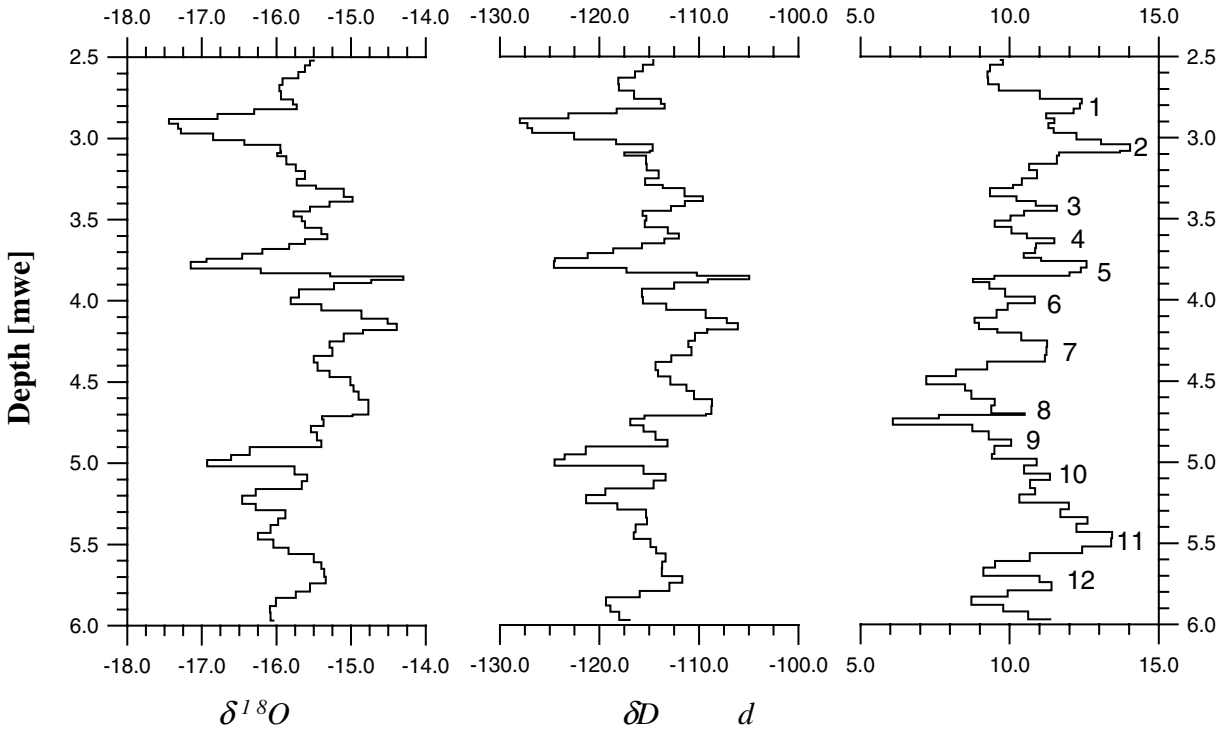


**Figure 8.** The distribution of $\delta^{18}O$, $\delta D$, and the deuterium excess $d$ over the ice depth interval 5–10 m. The interval contains 3.5 mwe, which suggests that there are ~10 annual cycles in this depth interval (based on the average accumulation rate of 0.36 mwe $yr^{-1}$). The deuterium excess shows 12 well-pronounced cycles, which may be annual cycles. Data are smoothed with a 3-point running mean. The 12 possible winter extremes are shown for the deuterium excess.

δD but show large variation for $d$ (relative to their mean values). The generally larger $\chi$ values for $d$ are a function of the way $d$ is derived ($d = \delta D - 8\delta^{18}O$). All series show a large average $\chi$ in the highest quartile, suggesting large sample-to-sample variations in the record. These parts may either be chronological hiatuses by wind erosion, climatological effects such as large precipitation events from isotopically anomalous air masses that have not been diffused fully into the average record, or examples of a few extreme events where the ice column shows transpositions of cycles by percolating meltwater. Since the average values are low, this suggests that most data do not feature these problems.

[40] The regression of the coisotopic relation was calculated to be $\delta D = 7.5\delta^{18}O + 2.7$. This is close to the globally averaged precipitation line, which has a slope of 8 [*Souchez and Lorrain*, 1991]. The δD record only extends over two depth intervals which yield regressions of $\delta D = 7.0\delta^{18}O - 5.0$ (5.0–10.2 m depth) and $\delta D = 7.8\delta^{18}O + 6.7$ (28.1–36.0 m depth).

[41] We also know that the precipitation line (and $d$) varies with time and space [e.g., *Vimeaux et al.*, 1999]. What is the annual and seasonal average value for $d$ in precipitated water at Lomonosovfonna? To estimate this, we use the isotope record from precipitation sampled at coastal stations on Spitsbergen. There are two available records: Isfjord Radio (78.07°N, 13.63°E, 6 m asl), covering parts of the period 1961–1975, and Ny-Ålesund (78.15°N, 11.56°E, 7 m asl), covering the period 1990–1997 [*International Atomic Energy Agency/World Meteorological Organization*, 1999]. The average precipitation line slopes from these stations were $\delta D = 7.2\delta^{18}O + 0.2$ (Ny-Ålesund) and $\delta D = 6.5\delta^{18}O - 6.0$ (Isfjord Radio). The $d$ calculated from $\delta^{18}O$ and δD is shown in Table 6. The data from these three different locations cover different periods; nevertheless, the ice core data are, on average, reasonably similar to the coastal station data. However, the ice core record does have a higher averaged $d$ (and precipitation line slope) than the coastal stations. This is probably explained by orographic effects [*Hoffmann et al.*, 1998]; since the ice core is taken at an elevation 1250 m higher than the coastal stations, the ice core data have been more distilled than the more "oceanic" signal that dominates the coastal stations. Other explanations may include geographical effects or the inflow of different air masses to the different sites.

[42] The tails of the distribution (assumed to be representative of winter and summer data) show smaller extremes in the ice core data than in the coastal data. This is primarily an effect of vapor-driven molecular diffusion of the extreme events in the snow pack and of downward smoothing by percolation events. It is generally known that short duration events in $\delta^{18}O$ and δD signals (storms) are rather quickly homogenized with time by vapor-driven diffusion [*Bolzan and Pohjola*, 2000] and that $d$ does not decrease with time as quickly as $\delta^{18}O$ since δD has a lower diffusion rate than $\delta^{18}O$ [*Johnsen et al.*, 2000]. During percolation events the isotope record is further smoothed, as shown by *Arnason et al.* [1973], with the degree of smoothing dependent on the amount of melting and percolation.

**Table 6.** Distribution of the Deuterium Excess $d$ From Different Records From Spitsbergen[a]

| | Ice Core | Ny-Ålesund 1990–1997 | Isfjord Radio 1961–1975 |
|---|---|---|---|
| Mean | 10.0 | 9.86 | 8.34 |
| $1Q$ | 8.7 | 4.98 | 3.85 |
| $4Q$ | 16.6 | 25.80 | 22.50 |

[a] Ny-Ålesund and Isfjord Radio are coastal stations at the sea level. The ice core record is from Lomonosovfonna summit at 1255 m asl. The record spans the depth interval 0–36 m, covering a time interval from 1997 back to about 1920s. $1Q$ and $4Q$ are the avearges of the first quartile (the 25% highest numbers) and of the fourth quartile (the 25% lowest numbers), respectively, of the distribution.

**Table 7.** Statistical Comparison of the Ice Core $\delta^{18}O$ Record From Lomonosovfonna Summit and Monthly Averages From the Global Network Isotopes in Precipitation Station at Ny-Ålesund[a]

| | Ice Core | Ny-Ålesund −4.8‰ |
|---|---|---|
| Average | −16.0 | −16.0 |
| Minima | −19.1 | −31.4 |
| Maxima | −12.0 | −10.2 |
| $1Q$ | −17.4 | −17.3 |
| $4Q$ | −14.8 | −14.5 |

[a] Ny-Ålesund covers 1990–1997. The ice core data is from the upper 6 meters of the ice core, which, from the number of $\delta^{18}O$ cycles, covers the period 1990–1997. The average value of Ny-Ålesund data was offset −4.8‰ to equalize the average with the ice core data. All values are in $\sigma^{18}O$ (‰ SMOW). $1Q$ and $4Q$ are the avearges of the first quartile (the 25% highest numbers) and of the fourth quartile (the 25% lowest numbers), respectively, of the distribution.

[43] To study the effects of diffusion on the record, we compared the $\delta^{18}O$ record from Ny-Ålesund (1990–1997) with the ice core record of that period. The 1989/1990 winter depth in the ice core was found by using the $\delta^{18}O$ cycles discussed in section 4. This placed the 1989/1990 winter layer at 5.3 m depth, corresponding to 2.55 mwe, which gives an average accumulation rate of 0.36 mwe $yr^{-1}$. We assumed a linear shift between the records owing to geographic and orographic gradients. The average value of the two series differed by 4.8‰. We also examined the isotopic altitude gradient by comparing the last winter's (1996/1997) accumulation in the record between the summit core and a core at lower elevation (core 5 at 750 m asl in Figure 1). The comparison gave an average altitudinal gradient of ∼0.1‰ 100 $m^{-1}$ over the ice field that winter. The offset between the Ny-Ålesund record and the summit ice core record was 4.3‰ in 1996/1997, which is close to the 4.8‰ difference estimated over the 7-year period above. The 1250-m elevation difference suggests that ∼25% of the offset between the Ny-Ålesund record and the ice core record from the summit is due to elevation effects, while the rest of the offset may then be due to geographical and topographical factors such as distance to sea, distance from mountains, etc. The gradient is rather low compared with, for example, Greenland (∼0.6‰ 100 $m^{-1}$) [*Zwally and Giovinetto*, 1997]; this may be due to the more maritime location of Lomonosovfonna. The availability of moisture around Spitsbergen due to the influence of the North Atlantic drift will lower the annual average of the isotopic cycle, damp the seasonal variations [*Hoffmann et al.*, 1998], and also damp the distillation function with altitude.

[44] In Table 7 we compare the distribution of the Ny-Ålesund $\delta^{18}O$ record with the record from the ice core that corresponds to the same period. After adjusting the Ny-Ålesund record to the 4.8‰ difference, we find that the lower and upper quartiles of the records are similar, although the total range of the distribution is much wider in the Ny-Ålesund data than the ice core record, related to the smoothing processes of the ice core record.

[45] Thus we find that the isotope record of the Lomonosovfonna summit ice core is well preserved albeit somewhat smoothed through percolation and vapor-driven diffusion. Percolation and refreezing of meltwater into ice layers in the firn have little effect, however, on the average distribution of the isotopes or on the cyclical nature and temporal distribution of the isotopes. The ice redistributed from percolation is transposed in depth/time, but it seems that most of the meltwater is refrozen within the annual layer. If not, we would not be able to find annual cycles, and we

would not be able to get an annual isotopic range in the ice core data that is similar to the range measured from precipitation at coastal stations.

## 6. Conclusions

[46] We have investigated the potential to derive meteoric precipitation signals from the periodically melting ice field Lomonosovfonna on Svalbard. Studying the available climatological data from the region, we find that the summit of the ice field is affected by melt most summers. Moreover, the available data suggest that the melt each summer varies between small to moderate amounts. We calculate a range of positive-degree days from 21 to 118°C d (1975–1995), which is estimated to give ~50% melt of the annual averaged accumulation during the warmest summer on record and ~25% melt in a median summer. The average melt index of ~55% in the core suggests an average melt of ~35% in this period, which falls within the calculated melt range. If last year's firn has an average porosity of 50%, then up to 50% melt can be accommodated within the pores in the firn. Thus most meltwater can be retained within the annual strata. Formation of ice lenses each winter, or during a summer cold snap, forms barriers to percolation between layers.

[47] Three diagnostics for the quality of the preservation of atmospherically deposited signals in the ice core record were investigated to study the amount of alteration affecting the record by percolating and refreezing meltwater. First we found that the most mobile ions, such as the anions associated with strong acids ($NO_3^-$ and $SO_4^{2-}$) showed up to 50% elution from firn layers and ~50% higher concentrations in ice. The most evenly distributed species was $NH_4^+$, which only shows ~10% variation between ice facies. A plausible reason for this is solid diffusion in the ice crystals after deposition. The least sensitive parameter was the water isotope, which had no detectable difference in distribution between the ice facies.

[48] The second diagnostic examined the distribution of peaks in the ionic concentrations of chemical species and the cyclicity in the water isotopes, the hypothesis being that all parameters had an annual cycle. The number of peaks/cycles showed that most parameters exhibited cycles and peaks close to that expected if an annual cycle was present. Indications are that the record suffers some dilution and diffusion but still preserves atmospherically deposited signals in their originally deposited strata.

[49] The third diagnostic concerned the quality of the least mobile parameter, the water isotope record. Statistical investigation of the water isotopes suggests that most of the record has a cyclic variation with depth, and percolating meltwater seems to have little importance in the reorganization of isotopic signals. Smoothing of the record is certainly present, but the location of the signal seems to be in situ. The water isotopes from the ice core were compared with water isotopes collected from precipitation at coastal stations on Spitsbergen. We found that the distribution of the isotopic records between the two different sites was similar after adjusting for a geographical gradient. The similarity between the ice core record and the coastal station record suggests that it is possible to recover a climatologically meaningful water isotope record from the summit of Lomonosovfonna.

[50] Our main conclusion, then, is that the upper part of this ice core holds a climatic and environmental record preserved with an annual or biannual resolution. Some of the most mobile ionic species will be eluted and transposed during the warmest years, but the peak signal will still be identifiable and most likely also retained within the seasonal layer. The least sensitive parameters such as water isotopes seem only slightly affected even during warm years. During periods cooler than the period 1920–1997 investigated here the record would be substantially less affected by percolation.

[51] **Acknowledgments.** We wish to thank the following: the Lomonosovfonna ice core 1997 field party for their efforts during the storms and snowmobile failures; the logistical division of the Norwegian Polar Institute, especially Einar Johansen; Håkan Samuelsson, Erik Huss, and Jüri Ivask for work on ice stratigraphy and sampling; Pierluigi Calanca and Jan Sedlacek for access to their climatic reconstructions; Ola Brandt for AWS rescue; Christian Jaedicke, Jemma Wadham, and the Norwegian Meteorological Institute for meteorological data; and Wibjörn Karlén and the Rovaniemi Finnish Forest Research Station for cold- and clean-room facilities. Stiftelsen Ymer-80, the Finnish Academy, the Swedish Natural Science Research Council, the Norwegian Polar Institute, the Estonian Ministry of Education, and the Nordic Council of Ministers all provided financial support. Finally, we thank Roy Koerner, Jack Kohler, and an anonymous referee, whose comments helped improve our manuscript.

## References

Arnason, B., T. Buason, J. Martinec, and P. Theodorsson, Movement of water through snow pack traced by deuterium and tritium, *IAHS Publ.*, *106*, 299–312, 1973.

Beine, H. J., M. Engardt, D. A. Jaffe, Ø. Hov, K. Holmén, and F. Stordal, Measurements of $NO_x$ and aerosol particles at the Ny-Ålesund Zeppelin mountain station on Svalbard: Influence of regional and local pollution sources, *Atmos. Environ.*, *30*(7), 1067–1079, 1996.

Benson, C. S., Stratigraphic studies in snow and firn of the Greenland Ice Sheet, *Folia Geogr. Danica*, *9*, 13–37, 1961.

Bolzan, J. F., and V. A. Pohjola, Reconstruction of the undiffused seasonal oxygen isotope signal in central Greenland ice cores, *J. Geophys. Res.*, *105*(C9), 22,095–22,106, 2000.

Braithwaite, R. J., Positive degree-day factors for ablation on the Greenland ice sheet studied by energy-balance modeling, *J. Glaciol.*, *41*(137), 153–160, 1995.

Dansgaard, W., Stable isotopes in precipitation, *Tellus*, *16*, 436–468, 1964.

Davies, T. D., C. E. Vincent, and P. Brimblecombe, Preferential elution of strong acids from a Norwegian ice cap, *Nature*, *300*, 161–163, 1982.

Gordienko, F. G., V. M. Kotlyakov, Y.-K. M. Punning, and R. Vaikmäe, Study of a 200-m core from the Lomonosov ice plateau on Spitsbergen and the paleoclimatic implications, *Polar Geogr. Geol.*, *5*(4), 242–251, 1981.

Goto-Azuma, K., S. Koshima, T. Kameda, S. Takahashi, O. Watanabe, Y. Fujii, and J. O. Hagen, An ice-core chemistry record from Snøfjellafonna, northwestern Spitsbergen, *Ann. Glaciol.*, *21*, 213–218, 1995.

Grumet, N. S., C. P. Wake, G. A. Zielinski, D. Fisher, R. Koerner, and J. D. Jacobs, Preservation of glaciochemical time series in snow and ice from Penny Ice Cap, Baffin Island, *Geophys. Res. Lett.*, *25*(3), 357–360, 1998.

Hara, K., K. Osada, M. Hayashi, K. Matsunaga, and Y. Iwasaka,Variation of concentrations of sulfate, methanesulfonate and sulfur dioxide at Ny Ålesund Ny-Ålesund in 1995/96 winter, *Proc. NIPR Symp. Polar Meteorol. Glaciol.*, *11*, 127–137, 1997.

Heintzenberg, J., and C. Leck, Seasonal variation of the atmospheric aerosol near the top of the marine boundary layer over Spitsbergen related to the Arctic sulphur cycle, *Tellus, Ser. B*, *46*, 52–67, 1994.

Hoffmann, G., M. Werner, and M. Heimann, Water isotope module of the ECHAM atmospheric general circulation model: A study on timescales from days to several years, *J. Geophys. Res.*, *103*(D14), 16,871–16,896, 1998.

International Atomic Energy Agency/World Meteorological Organization, Global network for isotopes in precipitation, GNIP database, release 3, Vienna, Austria, October 1999. (Available at http://www.iaea.org/programs/ri/gnip/gnipmain.htm.)

Isaksson, E., et al., A new ice core record from Lomonosovfonna, Svalbard: Viewing the data between 1920–1997 in relation to present climate and environmental conditions, *J. Glaciol.*, *47*(157), 335–345, 2001.

Johnsen, S. J., H. B. Clausen, K. M. Cuffey, G. Hoffmann, J. Schwander, and T. Creyts, Diffusion of stable isotopes in polar firn and ice: The isotope effect in firn diffusion, in *Physics of Ice Core Records*, edited by T. Hondoh, pp. 121–140, Hokkaido Univ. Press, Sapporo, 2000.

Koerner, R. M., Some comments on climatic reconstructions from ice cores drilled in areas of high melt, *J. Glaciol.*, *43*(143), 90–97, 1997.

Koerner, R. M., and D. A. Fisher, A record of Holocene summer climate from a Canadian high-Arctic ice core, *Nature*, *343*, 630–631, 1990.

Koerner, R. M., D. A. Fisher, and K. Goto-Azuma, A 100 year record of ion chemistry from Agassiz Ice Cap Northern Ellesmere Island NWT, Canada, *Atmos. Environ.*, *33*, 347–357, 1999.

Legrand, M., and P. Mayewski, Glaciochemistry of polar ice cores: A review, *Rev. Geophys.*, *35*(3), 219–243, 1997.

Nordli, P. Ø., I. Hanssen-Bauser, and E. J. Førland, Homogeneity analyses of temperature and precipitation series from Svalbard and Jan Mayen, *DNMI Rep. 16/96 Klima*, Norw. Meteorol. Inst., Oslo, 1996.

O'Dwyer, J., E. Isaksson, T. Vinje, T. Jauhiainen, J. Moore, V. Pohjola, R. Vaikmäe, and R. van de Wal, Methane sulfonic acid in a Svalbard ice core as an indicator of ocean climate, *Geophys. Res. Lett.*, *27*(8), 1159–1162, 2000.

Pasteur, E. C., and R. Mulvaney, Laboratory study of the migration of methane sulphonate in firn, *J. Glaciol.*, *45*(150), 214–218, 1999.

Petrenko, V. F., and R. W. Whitworth, *Physics of Ice*, 150 pp., Oxford Univ. Press, New York, 1999.

Pfeffer, W. T., and N. F. Humphrey, Determination of timing and location of water movement and ice-layer formation by temperature measurements in sub-freezing snow, *J. Glaciol.*, *42*(141), 292–304, 1996.

Pfeffer, W. T., and N. F. Humphrey, Formation of ice layers by infiltration and refreezing of meltwater, *Ann. Glaciol.*, *26*, 83–91, 1998.

Pinglot, J.-F., M. Pourchet, B. Lefauconnier, J. O. Hagen, E. Isaksson, R. Vaikmäe, and K. Kamiyama, Investigations of temporal change of the accumulation in Svalbard glaciers deducted from nuclear tests and Chernobyl reference layers, *Polar Res.*, *18*(2), 315–321, 1999.

Souchez, R. A., and R. D. Lorrain, *Ice Composition and Glacier Dynamics*, 207 pp., Springer-Verlag, New York, 1991.

Staebler, R., D. Toom-Sauntry, L. Barrie, U. Langendörfer, E. Lehrer, S. -M. Li, and H. Dryfhout-Clark, Physical and chemical characteristics of aerosols at Spitsbergen in the spring of 1996, *J. Geophys. Res.*, *104*(D5), 5515–5529, 1999.

Sun, J., D. Qin, P. A. Mayewski, J. E. Dibb, S. Whitlow, Z. Li, and Q. Yang, Soluble species in aerosol and snow and their relationship at Glacier 1, Tien Shan, China, *J. Geophys. Res.*, *103*(D21), 28,021–28,028, 1998.

Tarussov, A., The arctic from Svalbard to Severnaya Zemlya: Climatic reconstructions from ice cores, in *Climate Since A.D. 1500*, edited by R. S. Bradley and P. D. Jones, Routledge, New York, 1992.

Vimeaux, F., V. Masson, J. Jouzel, M. Stievenard, and J. R. Petit, Glacial-interglacial changes in ocean surface conditions in the Southern Hemisphere, *Nature*, *398*, 410–413, 1999.

Whillans, I. M., and P. M. Grootes, Isotopic diffusion in cold snow and firn, *J. Geophys. Res.*, *90*(D2), 3910–3918, 1985.

Zagorodnov, V. S., Recent Soviet activities on ice core drilling and core investigations in Arctic region, *Bull. Glacier Res.*, *6*, 81–84, 1988.

Zagorodnov, V. S., Correspondence: Comments on "Some comments on climatic reconstructions from ice cores drilled in areas of high melt" by Roy M. Koerner, *J. Glaciol.*, *44*(146), 191–193, 1998.

Zagorodnov, V. S., et al., Glubinnoye stroyeniye lednikovogo plato Lomonosova na o. Zap. Shpitsbergen, *Mater. Glyatsiologicheskikh Issled.*, *50*, 119–125, 1984.

Zwally, H. J., and M. B. Giovinetto, Areal distribution of the oxygen-isotope ratio in Greenland, *Ann. Glaciol.*, *25*, 208–213, 1997.

---

E. Isaksson, Norweigan Polar Institute, Polar Environmental Centre, N-9296 Tromsø, Norway. (elli@npolar.no)

T. Jauhiainen and J. C. Moore, Arctic Center, University of Lapland, Box 122, FIN-96101 Rovaniemi, Finland. ( jmoore@levi.urova.fi)

T. Martma and R. Vaikmäe, Institute of Geology, Tallinn Technical University, Estonia PST 7, 10143 Tallinn, Estonia.(martma@gi.ee; vaikmae@gi.ee)

H. A. J. Meijer, Centre for Isotope Research, Groningen University, Nijenborgh 4, 9747AG Groningen, Netherlands. (meijer@phys.rug.nl)

V. A. Pohjola, Department of Earth Sciences, Uppsala University, Villavägen 16, S-752 36 Sweden. (Veijo.Pohjola@natgeog.uu.se)

R. S. W. van de Wal, Institute of Marine and Atmospheric Research, Utrecht University, PO Box 80005, 3508TA Utrecht, Netherlands. (wal@phys.uu.nl)